Journal of
Ceramic Science
and Technology

*J. Ceram. Sci. Technol.*, **09** [1] 79-84 (2018)
DOI: 10.4416/JCST2017-00080
available online at: http://www.ceramic-science.com


# Enhanced Mechanical and Electromagnetic-Wave-Absorption Properties of Ceramic Matrix Composites Fabricated by Novel Laser-Machining-Assisted CVI

**J. Wang[1], Y. Liu[1], L. Cheng*[1], X. Chen[1], Q. Zhou[1], Z. Hou[1], F. Ye[1]**

[1]Science and Technology on Thermostructure Compsite Materials Laboratory, Northwestern Polytechnical University, Xi'an, Shaanxi, 710072, China

received October 10, 2017; received in revised form November 21, 2017; accepted January 16, 2018

**Abstract**

**A novel technique based on laser-machining-assisted chemical vapor infiltration (LA-CVI) was proposed and developed to fabricate ceramic matrix composites (CMCs). The results showed that the compressive strength, the shear strength and the bending strength of the C/SiC composites increased by 50.7 %, 11.8 % and 17.8 %, respectively, compared with those of classical CVI-C/SiC composites. The improvement can be attributed to the reopening of the diffusion channels and formation of a dense band and a coating around the channels. On the other hand, the minimum reflection loss (RL) of the C/SiC composites fabricated by means of LA-CVI improved 307 % against that of CVI-C/SiC composites in the frequency range of 8 GHz to 18 GHz owing to the multiple reflection of the electromagnetic (EM) waves in periodic micro-holes. The advantages of the LA-CVI method with regard to improving mechanical properties and the EM-wave-absorption properties of CMCs were demonstrated.**

*Keywords: Ceramic matrix composites, laser-machining-assisted CVI, mechanical properties, electromagnetic-wave-absorbing properties*

## I. Introduction

Ceramic matrix composites (CMCs) have received considerable attention in the aircraft, aerospace, wireless communication and military equipment sectors owing to their low density, high specific strength, excellent mechanical properties and good electromagnetic (EM)-wave-absorbing properties [1–4]. Three technologies have so far been developed for manufacturing CMCs: chemical vapor infiltration (CVI) [5], precursor infiltration pyrolysis (PIP) [6] and reactive melt infiltration (RMI) [7]. CVI, which facilitates the production of irregular-shaped components and avoids fiber damage at high temperature, has been effectively used to fabricate CMCs [8]. However, during CVI the gradients of temperature and flow field lead to inconsistent gas infiltration, consequently reducing the densification of the final composites.

To resolve this problem, a number of works based on the design of the preform structure, combining the advantages of CVI process, has been reported. John *et al.* [9] found that woven holes reflect a convolution of the effects of weave geometry and thus continue to contribute to the load-bearing capacity based on traditional CVI technology. Golecki [10] investigated surface "crusting" machining to meet the need to reopen the channels and reduce the density gradients to a minimum. Y. Hua *et al.* [11] have calculated the structure during CVI, especially the small pores among filaments and the large pores among bundles, which play a dramatic role in determining the deposition uniformity, processing time and final average density.

Most of the above works deal with cases that just describe phenomena in porous media of the preform, ignoring the micro-pores as the key factor to control the properties of CMCs. Accordingly, we propose a novel laser-machining-assisted chemical vapor infiltration (LA-CVI) to improve the qualities of CMCs, including the mechanical strength and EM-wave-absorbing properties, which can also provide useful insights and valuable guidelines for future CMC design.

In our previous work, femtosecond (fs) laser micromachining was successfully used to obtain a desirable porous structure of CMCs [12–14]. In this paper, emphasis was placed on evolution of the microstructure, strengthening mechanism and the enhancement of reflection loss (RL) for CMCs. The primary goal was to investigate whether the periodic microporous structure obtained with the LA-CVI process could contribute to the mechanical properties and EM-wave-absorbing properties of CMCs.

## II. Experimental Procedure

The preforms were densified in the LA-CVI process, which has been described in detail in our previous works [15]. In this study, we used C-fiber-reinforced SiC matrix composites (C/SiC) composites as an example of CMCs composites. Firstly, 2D preforms with fiber volume fraction of 40 % were fabricated. A thin pyrolytic carbon layer with a thickness of 200 nm was infiltrated on

* Corresponding author: chenglf@nwpu.edu.cn

the carbon fiber surface as the interfacial layer at 850 °C. Secondly, methyltrichlorosilane (CH3SiCl3, MTS) was used as a precursor for deposition of SiC matrix at 1100 °C for 260 h in a CVI reactor [16–17]. Thirdly, holes with the diameter of 0.6 mm and space of 5 mm were machined on the C/SiC under ambient conditions, using the beam delivered by a Ti:sapphire laser system (wavelength of 800 nm, repetition rate of 100 kHz, mean laser energy of 110 ± 10 μJ and pulse width 300 fs) [18]. Finally, after densification in a classic CVI furnace at 1100 °C for about 100 h, a thin SiC matrix layer was deposited on the surface of the holes and the C/SiC composite was formed by means of further densification.

The apparent density and open porosity of the samples were determined with the Archimedes' method. The microstructure's characteristics and the density distribution of the C/SiC fabricated by means of LA-CVI were determined in detail with microcomputed tomography (micro-CT, Y. Cheetah, YXLON, Germany) and scanning electron microscopy (SEM, S4700, Hitachi). The compressive strength, shearing strength and bending performance were all measured on a universal material testing system (Instron-1196). To depict the stress distribution of 2D C/SiC, the commercial software ANSYS was adopted for finite element modeling, using the 3D eight-node Solid 185 element to mesh the plates. The material properties are listed in Table 1 [19]. The RL of C/SiC composite was measured with a vector network analyzer (VNA; MS4644A, Anritsu, Japan) using the United States Naval Research Laboratory (NRL) arch free-space measurement method in the frequency range 8 GHz – 18 GHz [20].

## III. Results and Discussions

### *(1) Characterization of the C/SiC composites*

The densities, porosities and mechanical properties of the C/SiC composites fabricated by means of the conventional CVI process (denoted S1) and the LA-CVI process (denoted S2) are shown in Table 2. S2 obtained densities of 2.25 g·cm$^{-3}$, an improvement as high as 14.7 %, and the porosity of the C/SiC composites dropped to 23.7 % against S1. The increase in density could be attributed to the effect of micropores, which acted as deposition channels. During LA-CVI, once the deposition channels are reopened, the diffusion coefficient model can be calculated using the following equation [21].

$$D_B = D \cdot \frac{\varepsilon_B}{\tau_B} \quad (1)$$

where $D_B$ = binary diffusion coefficient, cm$^2$/s; D = diffusion coefficient, cm$^2$/s; $\varepsilon_B$ = porosity, %; $\tau_B$ = tortuosity. As the deposition channels increased, the pores including the micro-holes and the closed-holes inside opened; therefore, $\varepsilon_B$ and $D_B$ improved. Therefore, more MTS precursor can diffuse into the inner part of the preform, resulting in the increase in the density of the C/SiC composites.

Fig. 1 shows the density distribution the Micro-CT and SEM images of the C/SiC prepared via LA-CVI. As we see, the size of the micro-holes was almost the same as the pores between warp and weft tows (Fig. 1(a)). Fig. 1(b) shows that a dense band with 400 μm appeared, which reduced the porosity. Unlike the closed-pore marked in Fig. 1(c), the closed pores around the micro-holes were gradually filled with SiC matrix during further densification. Moreover, in the region around the hole, a coating with a thickness of about 50 μm and SiC particle measuring about 50 μm in diameter with spherical cauliflower-like shape can be observed (Fig. 1(d)). The formation of SiC can be described as follows:

$$CH_3SiCl_{3(v)} \xrightarrow{\text{excess } H_2} SiC_{(s)}\, 3HCl_{(v)} \quad (2)$$

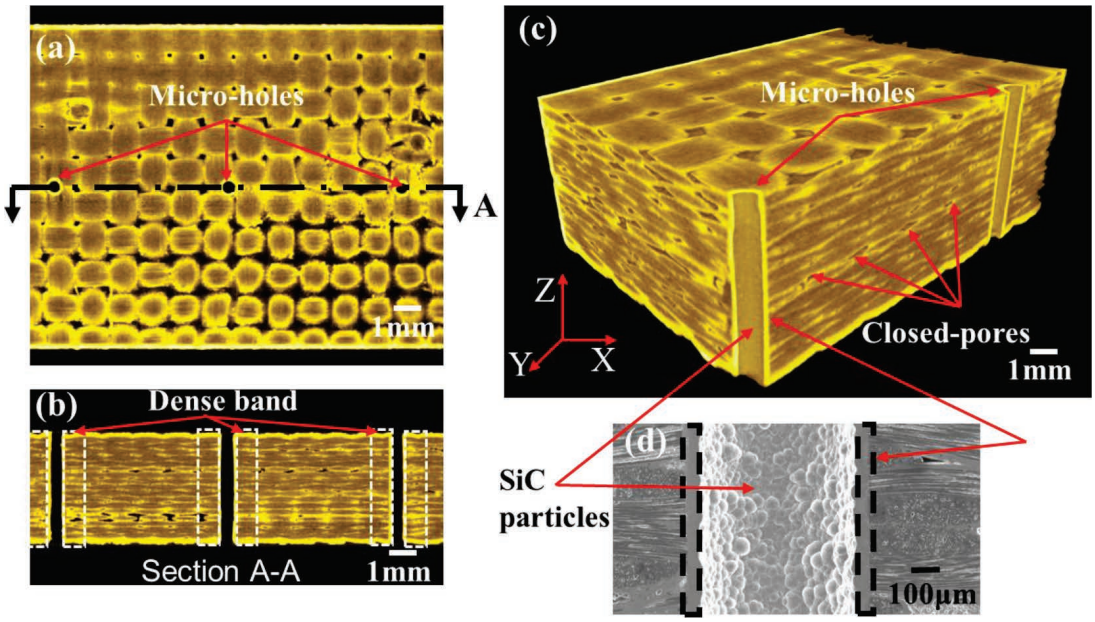


**Fig. 1:** Micro-CT and SEM images of 2D C/SiC: (a) Plan view of densified composite. (b) The cross-section along the depth direction of micro-holes. (c) 3D views of densified composite. (d) Magnification along the micro-hole in SEM.

**Table 1:** The mechanical properties of 2D C/SiC fabricated by CVI and LA-CVI.

| Technique | $E_1$ | $E_2$ | $E_3$ | $V_{12}$ | $V_{23}$ | $V_{13}$ | $G_{12}$ | $G_{23}$ | $G_{13}$ |
|---|---|---|---|---|---|---|---|---|---|
| | (GPa) | (GPa) | (GPa) | | | | (GPa) | (GPa) | (GPa) |
| CVI | 110 | 110 | 80 | 0.1 | 0.05 | 0.05 | 25 | 20 | 20 |
| LA-CVI | 142 | 142 | 112 | 0.1 | 0.05 | 0.05 | 45 | 41 | 41 |

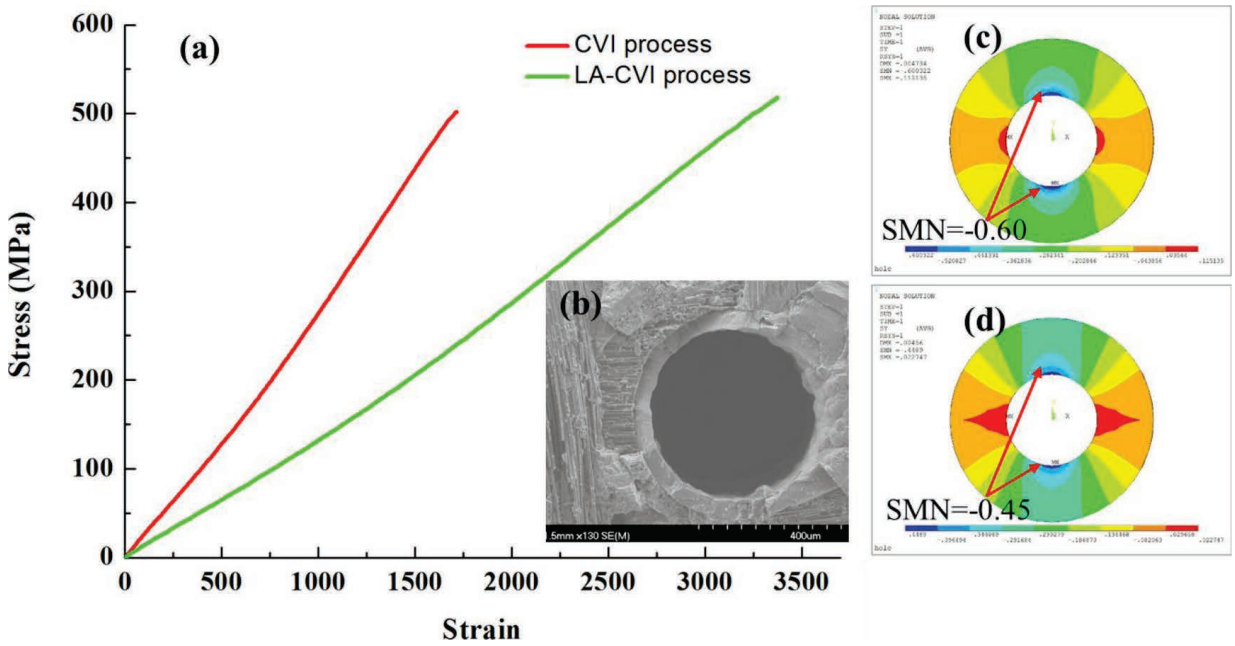


**Fig. 2:** The stress-strain curves and the fracture morphology of the sample prepared by CVI and LA-CVI under compressive loading: (a) Comparison of two curves; (b) micrograph of fracture surface; (c) distribution of the radial stress around the hole without further densified; (d) distribution of the radial stress around the hole under LA-CVI process.

**Table 2:** Characteristics of C/SiC composites fabricated by conditional CVI process and LA-CVI process.

| Sample | Density (g·cm-3) | Porosity (%) | Compressive Strength (MPa) | Shear strength (MPa) | Bending Strength (MPa) |
|---|---|---|---|---|---|
| Sl | 1.96 | 13.5 | 475±8 | 110±3 | 432±5 |
| S2 | 2.25 | 10.3 | 716±10 | 123±2 | 509±5 |

The newly SiC matrix is deposited on further densification. As we know, the theoretical density of CVI-SiC and SiC particles is 3.19 g/cm$^3$, which contributes to the improvement of mechanical strength [22]. Furthermore, with the attached SiC coating, the mechanical strength also increased [23].

### *(2) Mechanical properties of structural composites*

Generally speaking, the stress concentrating around the holes is caused by the holes, which further decreases the strength [24]. However, as shown in Table 1, compared to the CVI C/SiC, the compressive strength, the shear strength and the bending strength of the LA-CVI C/SiC improved by 50.7 %, 11.8 %, 17.8 % respectively.

Fig. 2 contrasts the stress-strain curves of the C/SiC composites prepared by means of CVI and LA-CVI under compressive loading, revealing the advantages of the LA-CVI process (Fig. 2(a)). Firstly, the higher density and higher content of SiC increased the fracture energy of the composites. And the SiC coating attached to the holes, acting as hollow pins, exhibited convoluted effects on crack propagation during the fracturing process (Fig. 2(b)) [25].

Secondly, based on comparison of the finite element method (FEM) results in Fig. 2(c) and 2(d), the stress concentration influence area of S2 is obviously smaller than that of S1 and the radial solution minimum (SNX) of S2 (SNX = -0.45) was clearly reduced compared with S1 (SNX = -0.60). That was to say, with further densification, the stress concentration of micro-holes had reduced dramatically under LA-CVI process, showing excellent damage tolerance and crack propagation resistance.

Fig. 3 shows the stress-strain curves of the C/SiC composites prepared by means of CVI and LA-CVI under shear loading, revealing the superiority of the LA-CVI process (Fig. 3(a)). On one hand, with the improvement in SiC matrix, the matrix crack was deflected and many long fibers were pulled out, as shown in Fig. 3(b). That verified that the shear strength was proportional to the number of matrix cracks, the width of the cracks and the length of debonding [26]. On the other hand, with further densification, the strain concentration around the micro-holes were reduced greatly. The maximum radial stress (SMX = 1.23) dropped compared with S1 (SMX = 1.86) and is illustrated in Fig. 2(c) and 2(d). Therefore, shear strength improved with LA-CVI, as listed in Table 1.

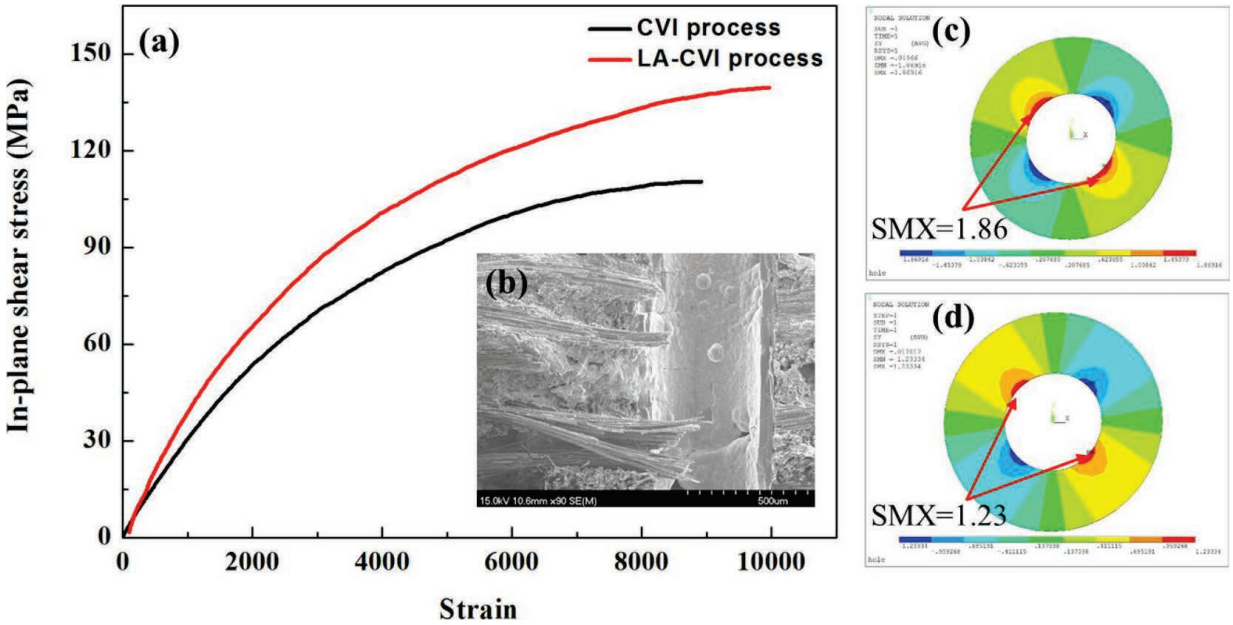


**Fig. 3:** The stress-strain curves and the fracture morphology of the sample prepared by CVI and LA-CVI under shear loading: (a) Comparison of two curves; (b) micrograph of fracture surface; (c) distribution of the radial stress around the hole without further densified; (d) distribution of the radial stress around the hole under LA-CVI process.

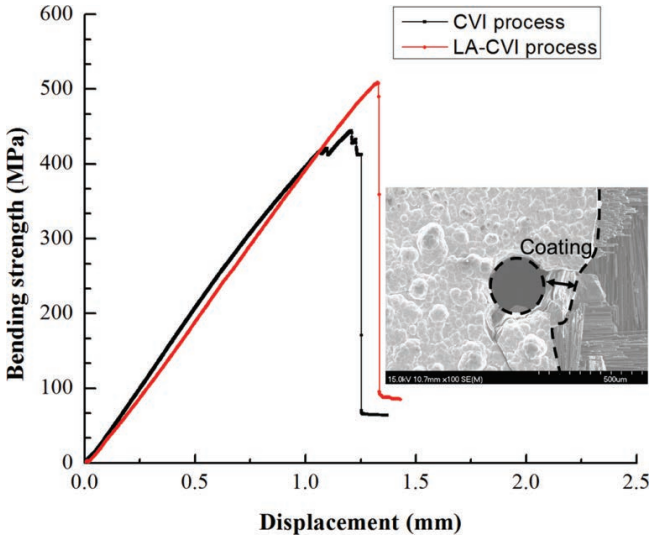


**Fig. 4:** The stress-displacement curves and the fracture morphology of the sample prepared by CVI and LA-CVI under bending force: (a) Comparison of two curves; (b) micrograph of fracture surface.

Fig. 4(a) shows the stress-displacement curves of the C/SiC composites prepared by means of CVI and LA-CVI when exposed to bending force. Fig. 4(b) was used to provide a direct readout of the damage mechanisms and failure mode of the material subjected to bending load. Firstly, many pull-out fibers are observed and not broken in one plane, which proved the damage tolerance of the composites. Secondly, on the fracture surface, crack propagation and branching and deflecting are also observed. Under bending force, the load is transferred efficiently from the rich matrix to the fiber, thus the excellent mechanical properties of the reinforcement are utilized, which is responsible for the enhanced flexural strength [27]. Last and most importantly, the crack propagation is not through the micro-hole, leading to a significantly higher capacity for damage tolerance and resistance to crack growth as a result of the coating adhering to the micro-hole (Fig. 4(b)). The new SiC coating was found to endow the C/SiC composite with improved strength [28]. Thus, with rich SiC matrix, nearly perfect bonded interface and SiC coating around the channel, the excellent mechanical properties of C/SiC composites prepared with the LA-CVI process are obtained, which is responsible for its enhanced flexural strength.

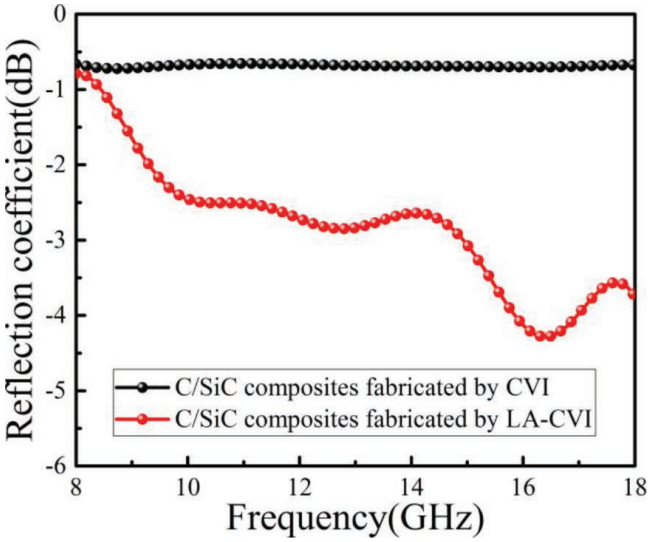


**Fig. 5:** RL as a function of frequency for C/SiC composites fabricated by CVI and LA-CVI.

### *(3) EM-wave-absorbing properties of the composite*

The microwave absorption of the absorption materials is usually represented by the RL of EM wave. Fig. 5 shows the RL of the C/SiCs depending on the fabrication process. It is shown that the C/SiC composites prepared by means of LA-CVI exhibit an excellent absorbing performance with an average RL of -2.81 dB, an improvement of 307 % on that of CVI with an average RL of -0.69 dB

at 8 GHz – 18 GHz. Owing to the formation of periodic micro-holes irradiated by the laser, the incident EM wave entering the composites is reflected many times in the ordered holes and propagates a much longer distance in random directions. Thus, the electromagnetic wave can be greatly scattered, altered and finally attenuated.This corresponds directly with the calculation above. Furthermore, according to the transmission line theory [29], the EM-absorbing property of the materials is evaluated based on RL, which can be characterized using the following expression:

$$RL = 10\log_{10}(P_R / P_I) \quad (dB) \qquad (3)$$

where $P_I$ and $P_R$ refer to incident power and received power of an EM wave, respectively. As seen from Eq. (3), when average RL is -0.69 dB, -2.81 dB respectively, while the absorbed EM power is 14.7 % and 47.6 %. That means more EM power is absorbed with an average RL of -2.81 dB.

## IV. Conclusions

LA-CVI has been confirmed to be an attractive technique for fabricating CMCs, resulting in an improvement of the mechanical properties and EM-wave-absorbing properties of CMCs. The compressive strength of the composites was increased by 50.7 %, the shear strength by 11.8 % and the bending strength by 17.8 %, respectively. Under compressive loading, the SiC coating fractured with the step circumferential shape was able to prevent cracks propagating. Under shear loading, the matrix crack showed damage-tolerant behavior with a strengthening of the matrix. Under bending load, crack propagation is blocked and deflected along the new SiC coating, which was able to yield a C/SiC composite with improved strength. The absorbing structure with periodic holes enhance multiple reflection and attenuation. The average RL increased by 307 %.

## Acknowledgement

The authors acknowledge the support of the Fund of the State Key Laboratory of Solidification Processing in NWPU (No. SKLSP201401), the Chinese National Foundation for Natural Sciences (No.51332004, No.51602257, No. 51672217), and the "111" project under Grant No. 08040.

## References

1 Naslain. R.: Design, preparation and properties of non-oxide CMCs for application in engines and nuclear reactors: an overview, *Compos. Sci. Technol.*, **64**, [2], 155 – 170, (2004).

2 Delhaes, P.: Chemical vapor deposition and infiltration processes of carbon materials, *Carbon*, **40**, [5], 641 – 657, (2002).

3 Qian, J., Wang, J., Hou, G., *et al.*: Preparation and characterization of biomorphic SiC hollow fibers from wood by chemical vapor infiltration, *Scripta Mater.*, **53**, [12], 1363 – 1368, (2005).

4 Yin, X., Kong, L., Zhang, L., *et al.*: Electromagnetic properties of Si-C-N based ceramics and composites, *Int. Mater. Rev.*, **59**, [6], 326 – 355, (2014).

5 Naslain, R.: CVI Composites, Warren Red. Ceramic Matrix Composites. London: Chapman and Hall, Blackie, 199 – 244, (1992).

6 Gonon, M., Fantozzi, G.: Densification of SiC/C/SiC composite materials by successive impregnation pyrolysis cycles with an organ metallic precursor, High Temperature Ceramic Matrix Composites, Woodhead, Bordeaux, 437 – 445, (1993).

7 Hillig, W.B.: Making ceramic composites by melt infiltration, *Am. Ceram. Soc. Bull.*, **73**, [4], 56 – 62, (1994).

8 Reznik, B., Gerthsen, D., Hüttinger, K.J.: Micro-and nanostructure of the carbon matrix of infiltrated carbon felts, *Carbon*, **39**, [2], 215 – 229, (2001).

9 Shaw, J.H., Rossol, M.N., Marshall, D.B., Zok, F.W.: Effects of tow-scale holes on the mechanical performance of a 3D woven C/SiC composite, *J. Am. Ceram. Soc.*, **98**, 948 – 956, (2015).

10 Golecki, I.: Rapid vapor-phase densification of refractory composites. *Mater. Sci. Eng.: R*, **20**, 37 – 124, (1997).

11 Feng, Y., Feng, Z., Li, S., Zhang, W., Luan, X., Liu, Y., Cheng, L., Zhang, L.: Micro-CT characterization on porosity structure of 3D Cf / SiCm composite, *Composites Part A: Appl. Sci. Manuf.*, **46**, [1], 133 – 141, (2009).

12 Jing, W., Chunhui, W., Yongsheng, L., Laifei, C., Weinan, L., Qing, Z., Xiaojun, Y.: Microstructure and chemical bond evolution of diamond-like carbon films machined by femtosecond laser, *Appl. Surf. Sci.*, **340**, 34 – 55, (2015).

13 Ruoheng, Z., Weinan, L., Yongsheng. L., Chunhui, W., Jing, W., Xiaojun, Y., Laifei, C.: Machining parameter optimization of C/SiC composites using high power pico-second laser, *Appl. Surf. Sci.*, 330, 321 – 331, (2015).

14 Yongsheng, L., Jing, W., Weinan, L., Chunhui. W., Qing, Z., Xiaojun, Y., Laifei, C.: Effect of energy density and feeding speed on micro-holes drilling in SiC/SiC composites by picosecond laser, *Int. J. Adv. Manuf. Tech.*, **84**, [9], 1917 – 1925, (2016).

15 Jing, W., Laifei, C., Yongsheng, L., Litong, Z., Xiaoying, L., Yi, Z., Qing. Z.: Enhanced densification and mechanical properties of carbon fiber reinforced silicon carbide matrix composites via laser machining aided chemical vapor infiltration, *Ceram. Int.*, **43**, 11538 – 11541, (2017).

16 Xu, Y.D., Cheng, L.F., Zhang, L.T., Yin, H.F., Yin, X.W.: Microstructure and mechanical properties of three-dimensional textile hi-nicalon SiC/SiC composites by chemical vapor infiltration, *J. Am. Ceram. Soc.*, **85**, [5], 1217 – 1221, (2002).

17 Mei, H., Cheng, L.F., Zhang, L.T., Luan, X.G., Zhang, J.: Behavior of two-dimensional C/SiC composites subjected to thermal cycling in controlled environments, *Carbon*, **44**, [1], 121 – 127, (2006).

18 Yongsheng, L., Chunhui, W., Weinan, L., Xiaojun, Y., Qing, Z., Laifei, C., Litong, Z.: Effect of energy density on the machining character of C/SiC composites by picosecond laser, *Appl. Phys. A*, 116, [3], 1221 – 1228, (2013).

19 Zongbei, H., Litong, Z., Yi, Z., Yongsheng, L., Xiaoying, L., Bo, C.: Microstructural characterization and failure analysis of 2D C/SiC two-layer beam with pin-bonded hybrid joints, *Int. J. Adhes. Adhes.*, 57, 70 – 78, (2015).

20 Yin, X., Xue, Y., Zhong, L., Cheng, L.; Dielectric, electromagnetic absorption and interference shielding properties of porous yttria-stabilized zirconia/silicon carbide composites, *Ceram. Int*., **38**, 2421 – 2427, (2012).

21 Nowak, B., Karlström, O., Backmann, P., Brink, A. Zevenhoven, M., Voglsam, S., Winter, F., Hupa, M.: Mass transfer limitation in thermogravimetry of biomass gasification, *J. Therm. Anal. Calorim.*, **111**, [1], 183 – 192, (2013).

22 Yunfeng, H., Litong, Z., Laifei, C., Zhengxian, L., Jihong, D.: Microstructure and mechanical properties of $SiC_P$/SiC and $SiC_W$/SiC composites by CVI, *J. Mater. Sci.*, **45**, 392 – 398, (2010).

23 Hwan-Sup, L., Jun-Gyu, K., Doo-Jin, C.: The effects of SiC whiskers and an SiC film coating deposited by chemical vapor infiltration (CVI) on a porous cordierite substrate, *J. Mater. Sci.*, **43**, 5574 – 5578, (2008).

[24] Nakai, A., Ohki, T., Takeda, N., Hamada, H.: Mechanical properties and micro-fracture behaviors of flat braided composites with a circular hole, *Compos. Struct*, **52**, 315 – 322, (2001).

[25] Suo, T., Fan, X., Hu, G. *et al.*: Compressive behavior of C/SiC composites over a wide range of strain rates and temperature, *Carbon*, **62**, 481 – 492, (2013).

[26] Guo, H.B., Wang, B., Jia, P.R. *et al.*: In-plane shear behaviours of a 2D-SiC/SiC composite under various loading conditions, *Ceram. Int.*, **41**, 11562 – 11569, (2015).

[27] Yang, W.: Development of CVI process and property evaluation of CVI-SiC/SiC composites, Doctoral thesis, Institute of Advanced Energy, Kyoto University, (2002).

[28] Liang, J., Xiao, H., Gao, P. *et al*.: Microstructure and properties of 2D-Cf/SiC composite fabricated by combination of CVI and PIP process with SiC particle as inert fillers, *Ceram. Int.*, **43**, [2], 1788 – 1794, (2017).

[29] Yin, X.W., Cheng, L.F., Zhang, L.T., Travitzky, N., Greil. P.; Fibre-reinforced multifunctional SiC matrix composite materials, *Int. Mater. Rev.*, **62**, [3] 117 – 172, (2017).